JACS
JOURNAL OF THE AMERICAN CHEMICAL SOCIETY
Article
pubs.acs.org/JACS

Mechanistic Investigation of the Palladium-Catalyzed Synthesis of Allylic Silanes and Boronates from Allylic Alcohols

Johanna M. Larsson and Kálmán J. Szabó*

Department of Organic Chemistry, Stockholm University, SE-106 91 Stockholm, Sweden

Supporting Information

ABSTRACT: The mechanism of the palladium-catalyzed synthesis of allylic silanes and boronates from allylic alcohols was investigated. ^{1}H, ^{29}Si, ^{19}F, and ^{11}B NMR spectroscopy was used to reveal key intermediates and byproducts of the silylation reaction. The tetrafluoroborate counterion of the palladium catalyst is proposed to play an important role in both catalyst activation as well as the transmetalation step. We propose that BF_3 is generated in both processes and is responsible for the activation of the substrate hydroxyl group. An (η^3-allyl)palladium complex has been identified as the catalyst resting state, and the formation of (η^3-allyl)palladium complexes directly from allylic alcohols has been studied. Kinetic analysis provides evidence that the turnover limiting step is the transmetalation, and insights into notable similarities between the borylation and the silylation reaction mechanisms enabled us to considerably improve the stereoselectivity of the borylation.

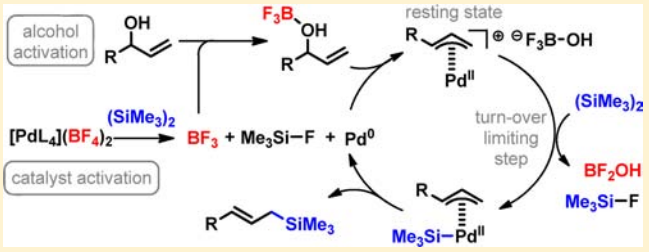

INTRODUCTION

The direct activation of allylic alcohols in transition metal catalysis has recently emerged as an attractive approach for the formation of new carbon−carbon and carbon−heteroatom bonds.[1,2] From an economic perspective, these stable and readily available substrates are preferable to the more commonly used allylic carboxylates, carbonates, and halides, which are themselves usually prepared from the corresponding allylic alcohols.[1b,c,2f]

Allylic silanes and allylic boronates are important building blocks in modern organic synthesis.[3] Their low toxicity and relatively high stability make them extremely useful reagents in the regio- and stereoselective allylation of electrophiles[3h,4] as well as useful transmetallating reagents in transition-metal-catalyzed reactions, such as Hiyama or Suzuki−Miyaura couplings.[3h,5,6] As a result, considerable effort has gone into the development of attractive methods for the preparation of organo silanes and boronates using transition metal catalysis.[7]

We have previously reported the palladium-catalyzed conversion of allylic alcohols to allylic boronates under mild conditions[2b,8] (Scheme 1) and shown that these reagents can be used subsequently in allylation reactions to form stereodefined homoallylic alcohols and amines[9] as well as cross-coupling products with unusual regioselectivity.[10] Recently, we showed that the commercially available palladium complex $[Pd(MeCN)_4](BF_4)_2$ (**3**) catalyzes the borylation at lower temperatures with shorter reaction times. Importantly, we found that replacing the boron source with $(SiMe_3)_2$ (**2**) in this system enables the unprecedented conversion of allylic alcohols directly to the corresponding silanes in good yields (Scheme 2).[2a] Both reactions proceed with remarkably high regio- and stereoselectivity to afford the linear allylic products with *trans* configuration. Previous methods published by Miyaura, Tsuji, and Lipshutz for the synthesis of allylic silanes and boronates

Scheme 1. Synthesis of Allylboronates from Allylic Alcohols Using Pincer Complex Catalysis Developed by the Szabó Group (L = SePh, X = Cl; L = SMe, X = BF_4^-)[2b,8]

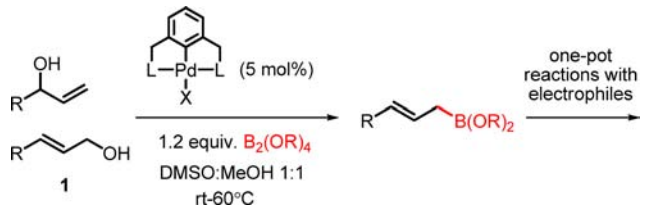

Scheme 2. Pd(II)-Catalyzed Silylation and Borylation of Allylic Alcohols under Mild Conditions Developed by the Szabó Group[2a]

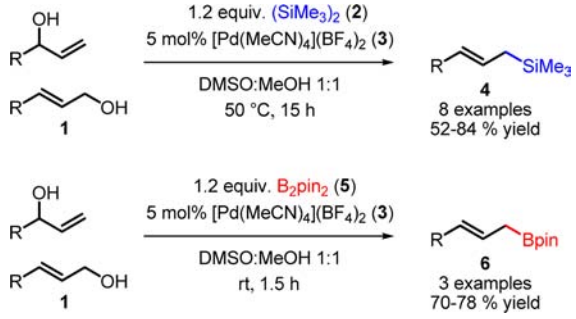

Received: October 5, 2012
Published: November 30, 2012

   dx.doi.org/10.1021/ja309860h | J. Am. Chem. Soc. 2013, 135, 443−455

have required preinstalled leaving groups, such as acetates or trifluoroacetates.[7b,d,e]

In our system, allylic alcohols underwent silylation much faster than did allylic acetates[2a]—a surprising result given the poor nucleofugicity of the hydroxyl group. This result, and the fact that silylation and borylation of allylic alcohols have not yet been studied in detail, inspired us to undertake a mechanistic investigation. It was previously found that the silylation and borylation behave similarly in many respects.[2a] In both reactions $[Pd(MeCN)_4](BF_4)_2$ was shown to be the most efficient catalyst source. Addition of more strongly coordinating ligands such as phosphines, LiCl, and LiOAc were found to inhibit both reactions. Furthermore, both the silylation and the borylation proceed faster with allylic alcohols as substrates than with allylic acetates.

We focused on the catalytic performance of $[Pd(MeCN)_4](BF_4)_2$, which proved to be the most reactive catalyst in our previous studies. In particular, attention was directed to the following aspects:

- How is the hydroxyl group activated?
- What is the key organopalladium intermediate of the reaction?
- What is the turnover limiting step of the reaction?
- What are the similarities and differences between the silylation and borylation reactions?

We initially chose to investigate the silylation reaction, given the higher stability of the allylic silane products compared to the allylic boronate products. The silylation is also slower, making it a more obvious choice for easier spectroscopic detection of intermediates as well as kinetics experiments.

In this study, we show that the tetrafluoroborate anion releases BF_3, which is able to activate allylic alcohol substrates. We identify (η^3-allyl)palladium species as key intermediates and find that transmetalation is the rate-limiting step for the silylation. Similarities between the silylation and borylation reactions allow for a substantial improvement in the diastereoselectivity of the borylation.

RESULTS AND DISCUSSION

As a model reaction, we chose the silylation of commercially available **1a**, for which the reaction is clean, is high yielding, and gives a stable product. Deuterated solvents were used for ease of analysis (Scheme 3).

Scheme 3. Model Reaction for Studying the Silylation Reaction of Allylic Alcohols[2a]

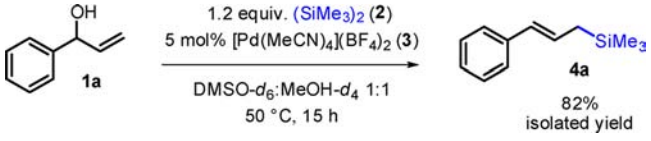

Multinuclear NMR Analysis. We sought initial insights by examining reaction intermediates and byproducts. To start, the course of the silylation of **1a** (Scheme 3) was followed by ^{29}Si NMR spectroscopy. During the reaction the consumption of $(SiMe_3)_2$ (**2**) and the formation of the silylated product (**4a**) were observed throughout (Figure 1 shows the ^{29}Si NMR spectrum of the mixture at the end of the reaction; see Figure S1 in the Supporting Information for changes observed over time).

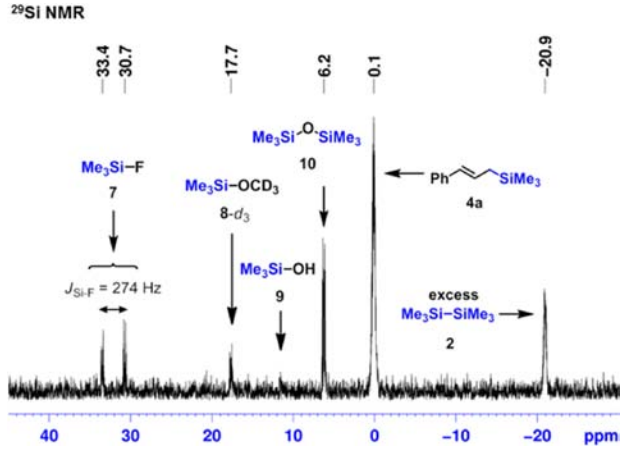

Figure 1. ^{29}Si NMR spectrum of the crude reaction mixture after complete conversion of **1a** to **4a** (Scheme 3).

After 1.5 h Me_3Si-OD_3 (**8**-d_3) appeared, and after 2.5 h a small peak corresponding to Me_3Si−OH (**9**) (11.60 ppm) was also observed. Thereafter, the concentration of **8** and **9** started decreasing, due to the formation of hexamethyldisiloxane (**10**) (Scheme 4) which is observed 4 h after the start of the reaction (Figure S1, Supporting Information).[11]

Scheme 4. Condensation of 8-d_3 and 9 Forming 10

Except the ^{29}Si NMR signals of **8**-d_3, **9**, and **10**, 15 min after starting the reaction a doublet at 32 ppm (J_{Si-F} = 274 Hz) was observed (Figure S1, Supporting Information), which was identified as the resonance signals of Me_3Si−F (**7**). This was a surprising finding, as the BF_4^- catalyst counterion was the only possible fluorine source present in the reaction mixture. Me_3Si−F formed rapidly at an early stage of the reaction, and its amount continuously increased during the time the reaction was monitored (11 h, Figure S1, Supporting Information).

To find out more about the role of BF_4^-, the reaction was also monitored by ^{19}F NMR spectroscopy (Figure 2 shows the

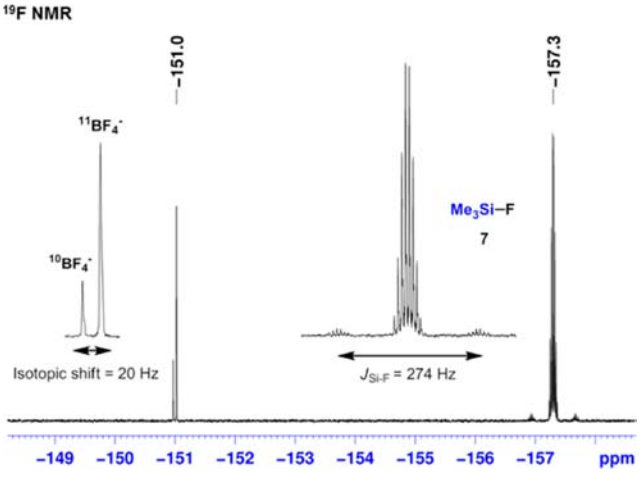

Figure 2. ^{19}F NMR spectrum of the crude reaction mixture after complete conversion of **1a** to **4a** (Scheme 3).

dx.doi.org/10.1021/ja309860h | J. Am. Chem. Soc. 2013, 135, 443−455

^{19}F NMR spectrum of the mixture at the end of the reaction; see Figure S2 in the SI for changes observed over time). As boron has two naturally occurring isotopes, ^{10}B (20% natural abundance) and ^{11}B (80% natural abundance), compounds containing B−F bonds are easily identifiable in ^{19}F NMR spectroscopy where F−^{10}B and F−^{11}B give rise to two peaks in close proximity to each other in a 1:4 ratio (e.g., see signals of BF_4^- in Figure 2).[12] At the start of the reaction formation of BF_3 (**11**) was observed.[13] After 10 min, the concentration reached its maximum and then started decreasing. After 2 h the concentration of BF_3 was too low to be observed. However, the tetrafluoroborate anion continued being consumed, suggesting that BF_3 is formed throughout the reaction (Figure S2 in the SI). At the end of the reaction, 5% of BF_4^- still remained.

Likewise, the ^{11}B NMR spectrum of this mixture showed a small amount of BF_4^- still present and also that the remainder of the boron-containing compounds was in the form of $B(OR)_3$ (Figure 3). The broad, partially overlapping peaks at 18.5 and

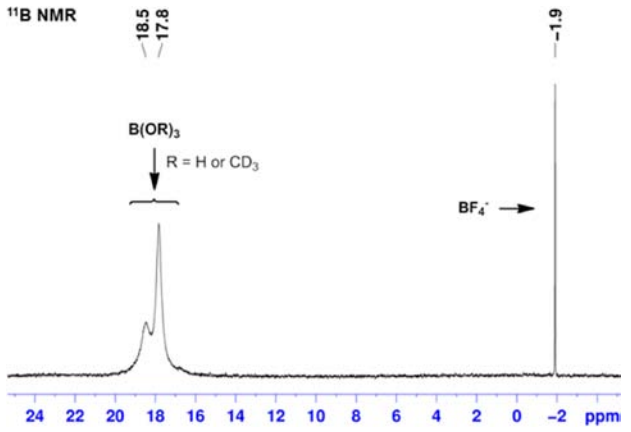

Figure 3. ^{11}B NMR spectrum of the crude reaction mixture after complete conversion of **1a** to **4a** (Scheme 3).

17.8 ppm correspond to the equilibrium between $B(OH)_3$ and $B(OCD_3)_3$ in the DMSO-d_6/MeOH-d_4 solvent mixture, as verified by comparing against genuine samples of $B(OMe)_3$ and $B(OH)_3$. The tetrafluoroborate anion is known to undergo slow hydrolysis in aqueous solution.[14] We therefore investigated the stability of the counterion of the palladium catalyst **3** in the solvent mixture. Accordingly, **3** was heated at 50 °C in a 1:1 mixture of DMSO-d_6 and MeOH-d_4 for 15 h, at which time ^{19}F NMR analysis of the solution did not show appreciable changes. Palladium black formation could not be observed, and formation of hydrogen fluoride (HF) was not detected. The catalytic model reaction was also repeated in a Teflon-lined NMR tube. However, even though the direct contact of HF with the glass surface was prevented, evolution of HF could not be observed.

Intermediate Formation of Allylic Ether 12. Running our model reaction (Scheme 3) at room temperature instead of 50 °C for 15 h gave a product mixture containing allylic silane **4a**, linear allylic ether **12a**-d_3, and a small amount of **12b**-d_3 (Scheme 5). Also, if the model reaction at 50 °C is stopped after 3 h, before full conversion to **4a**, formation of **12a**-d_3 and **12b**-d_3 can be observed by ^{1}H NMR spectroscopy. However, after 15 h they are fully consumed. We therefore wanted to find out which role these possible intermediates play in the silylation reaction. Running our model reaction without disilane **2** for 15

Scheme 5. Model Silylation Reaction Performed at Room Temperature[a]

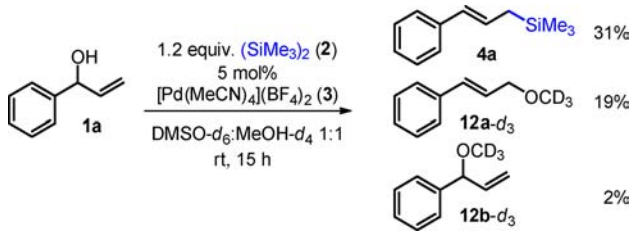

[a]The yields are determined by ^{1}H NMR spectroscopy using an internal standard.

h gave full conversion to the allylic ethers (Scheme 6). The linear ether (**12a**-d_3) was formed in 87% NMR yield together

Scheme 6. Sequential Etherification−Silylation[a]

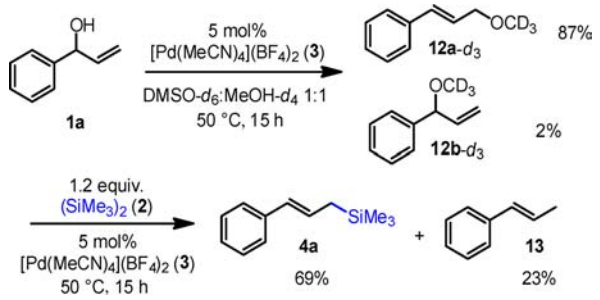

[a]The yields are determined by ^{1}H NMR spectroscopy using an internal standard.

with a small amount of branched ether (**12b**-d_3). The addition of $(SiMe_3)_2$ to the crude mixture of this reaction and heating for a further 15 h at 50 °C led only to a low conversion (35%) to allylsilane **4a** due to decomposition of the palladium catalyst. By contrast, when both $(SiMe_3)_2$ and a new portion of palladium catalyst **3** (5 mol %) were added to the crude reaction mixture (which was then heated for 15 h) ethers **12a**-d_3 and **12b**-d_3 were consumed, and allylsilane **4a** was formed in 69% NMR yield together with **13** (23% NMR yield) (Scheme 6). It is important to point out that a much smaller amount of **13** (approximately 2%) was detected during our model reaction (Scheme 3).

To test whether Pd(0) might be responsible for the high yield of byproduct **13** in the sequential reaction, **12a** was used directly as a substrate in the silylation (Scheme 7). Under the standard conditions **12a** was converted to **4a** in high NMR yield, and the formation of **13** became comparable to that of

Scheme 7. Model Silylation Reaction Performed Using 12a as a Substrate[a]

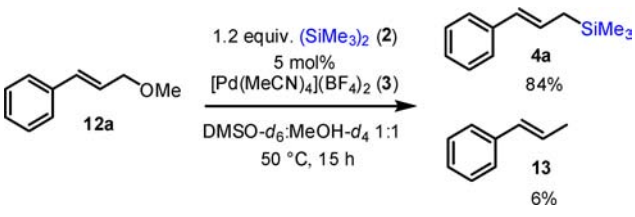

[a]The yields are determined by ^{1}H NMR spectroscopy using an internal standard.

dx.doi.org/10.1021/ja309860h | J. Am. Chem. Soc. 2013, 135, 443−455

our model reaction (6% NMR yield). This finding suggests that the formation of **13** is promoted by Pd(0) (see discussion below).

Having established that allylic ether **12a** can be converted to silane **4a**, we sought to establish the extent of ether formation in our model reaction. Thus, a competition experiment between allylic alcohol **1a** and allylic ether **12a** under the conditions of our model reaction was followed by ^{1}H NMR spectroscopy for 13 h (Figure 4). As MeOH-d_4 acts as the only

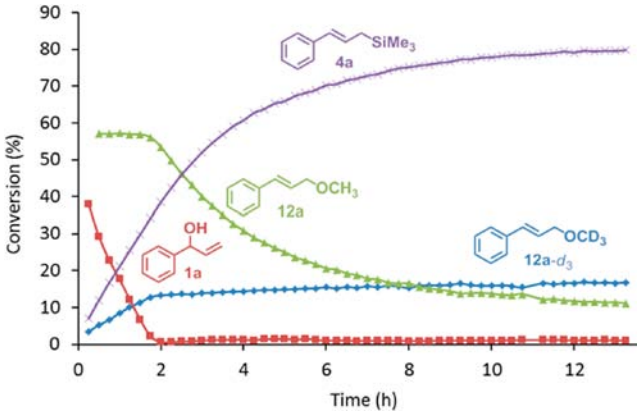

Figure 4. Competitive silylation reaction using **12a** and **1a** as starting materials. Lines are given as a guide for the eye.

source of $-OCD_3$, the use of nondeuterated **12a** enabled easy differentiation between starting material (**12a**) and product (**12a**-d_3) ethers. The allylic alcohol **1a** was consumed rapidly, and the conversion of **12a** was observed to begin only after **1a** was completely consumed. This shows that silane **4a** is not exclusively produced via ether **12a**. In addition, silane **4a** is formed at a higher rate than **12a**-d_3, suggesting that **4a** is mainly formed directly from **1a**. The finding that ether **12a**-d_3 is formed from both **1a** and **12a** indicates that **12a**-d_3 may be a common intermediate in conversion of both **1a** and **12a**. The relatively constant concentration of **12a**-d_3 after 2 h is the result of two opposing processes. The concentration of allylic ether **12a**-d_3 increases due to the formation from **12a**, while at the same time **12a**-d_3 is consumed by transformation to silane **4a**. The formation of **12a** from **12a**-d_3 is not observed due to the considerably higher concentration of CD_3OD compared to that of CH_3OH.

Activation of the Hydroxyl Group. Replacement of **3** with 2.5 mol % $Pd_2(dba)_3$ (**14**) (dba = dibenzylideneacetone) in our model reaction (Scheme 3) changed the outcome substantially (Scheme 8). Only 2% linear ether **12a**-d_3 was formed, and the rest of the allylic alcohol **1a** remained unreacted. This subcatalytic process (Scheme 8) was

Scheme 8. Attempted Silylation Using $Pd_2(dba)_3$ as Catalyst[a]

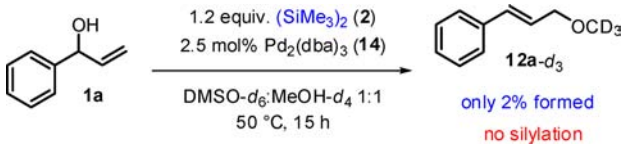

[a]The yield is determined by ^{1}H NMR spectroscopy using an internal standard. dba = dibenzylideneacetone.

accompanied with formation of Pd black. Previous work by Tamaru has shown that Pd(0) can catalyze allylic alcohol substitutions, albeit always in the presence of a Lewis acid, such as BEt_3.[1a,15] We therefore reasoned that BF_3, whose presence in our model reaction (using **3** as catalyst, Scheme 3) we demonstrated above, may be of key importance for the activation of the hydroxyl group. Indeed, when we conducted the reaction shown in Scheme 8 in the presence of 15 mol % of $BF_3{\cdot}OEt_2$, it afforded allylic silane **4a** in 72% NMR yield together with 14% **12a**-d_3 (Scheme 9). This finding clearly

Scheme 9. Silylation Using $Pd_2(dba)_3$ and $BF_3{\cdot}OEt_2$ as Catalysts[a]

[a]The yields are determined by ^{1}H NMR spectroscopy using an internal standard.

shows that a catalytic amount of BF_3 is able to activate efficiently the hydroxyl group toward palladium-catalyzed substitution under conditions very similar to our model reaction.

As expected, silylation did not occur in the absence of palladium, even in the presence of $BF_3{\cdot}OEt_2$ (Scheme 10). However, **12a**-d_3 and **12b**-d_3 did form, presumably either via a less regioselective S_N2/S_N2' and/or S_N1 mechanism.

Scheme 10. Attempted Silylation without Palladium Catalyst[a]

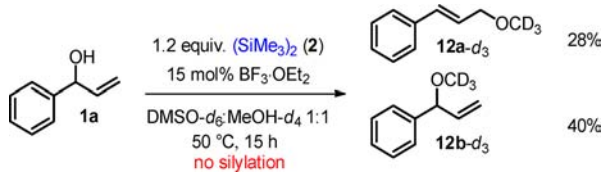

[a]The yields are determined by ^{1}H NMR spectroscopy using an internal standard (a reaction profile can be found in the Supporting Information).

Resting State of the Catalyst. When the course of our model silylation reaction (Scheme 3) was monitored by ^{1}H NMR spectroscopy, a fast forming species [**15**L_2]−X was observed (Figure 5b). The corresponding signals were also observed in previous experiments, such as the silylation of cinnamyl alcohol **1b** (Figure 5c) and allylic ether **12a**. Species [**15**L_2]−X was present at a constant concentration throughout the reaction. Its ^{1}H NMR spectrum displays the characteristic coupling pattern and shift values of (η^3-allyl)palladium complexes, such as (**15**-Br)$_2$ (Figure 5a).[16] On the basis of a possible intermediacy of (η^3-allyl)palladium species in our model reaction (Scheme 3) and the presence of tetrafluoroborate in **3**, the new signals are expected to belong to a (η^3-allyl)palladium−BF_4 complex. Therefore, we separately synthesized complex [**15**L_2]−BF_4. Halide abstraction of (**15**-Br)$_2$ using $AgBF_4$ in DMSO-d_6/MeOH-d_4 (Scheme 11) gave (η^3-allyl)palladium complex [**15**L_2]−BF_4. The ^{1}H NMR shift values and coupling constants of [**15**L_2]−BF_4 are in good agreement

dx.doi.org/10.1021/ja309860h | J. Am. Chem. Soc. 2013, 135, 443−455

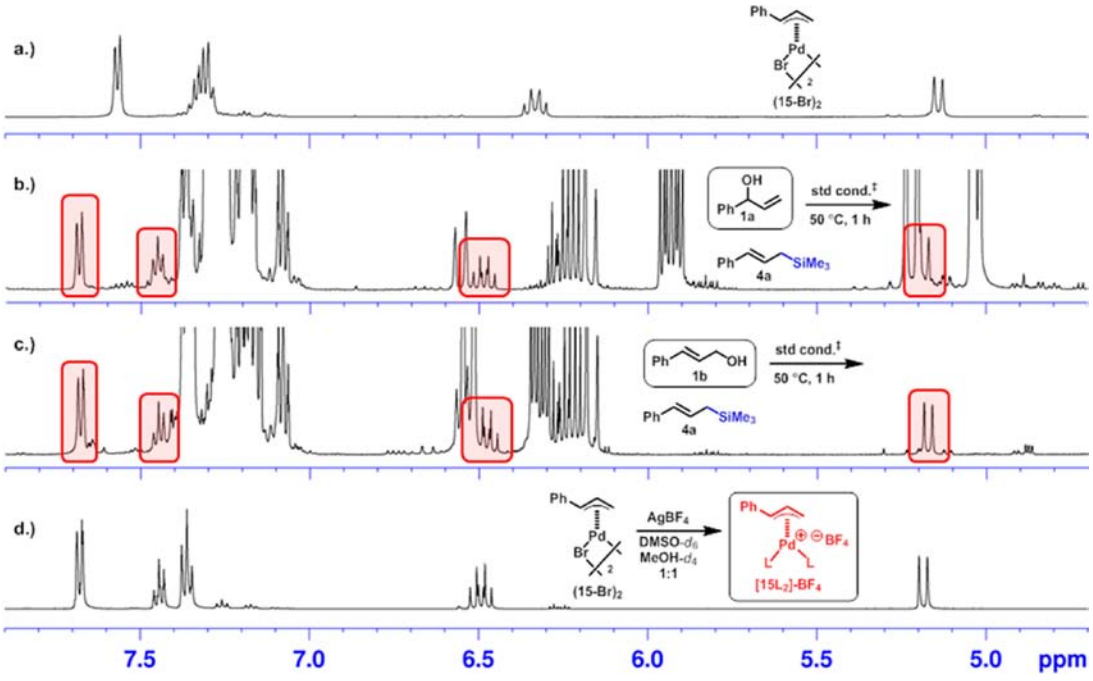

Figure 5. ^{1}H NMR spectra of the silylation of **1a** (b) and **1b** (c) after 1 h and authentic samples of (η^3-allyl)palladium complexes (**15**−Br)$_2$ (a) and [**15**L$_2$]−BF$_4$ (d) in DMSO-d_6/MeOH-d_4 1:1 solutions. ‡std cond. (standard conditions, reaction arrows in **5**b,c): 1.2 equiv of **2**, 5 mol % **3**, DMSO-d_6/MeOH-d_4 1:1.

Scheme 11. Ligand Exchange of Complex [15L$_2$]−BF$_4$

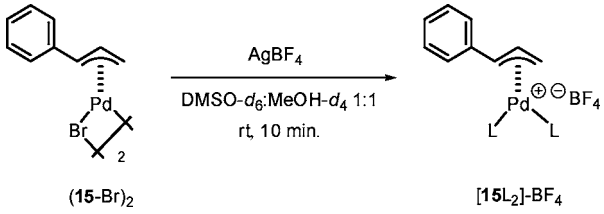

with those of the species observed during catalysis (compare Figures 5b,c with 5d). Therefore, we assign the newly observed peaks to the (η^3-allyl)palladium complex [**15**L$_2$]−BF$_4$ or, given the reactivity and weak coordinating ability of BF_4^-, a very closely related cationic species.

Fluorine−carbon coupling was not observed for the allylic fragment in complex [**15**L$_2$]−BF$_4$ by ^{13}C NMR spectroscopy, consistent with the fact that BF_4^- is a counterion in complex [**15**L$_2$]−BF$_4$. The exact nature of this (η^3-allyl)palladium complex in DMSO-d_6/MeOH-d_4 solution has not been determined. Since BF_4^- is known to be a weakly coordinating ligand, the complex is assumed to be cationic. In the reaction mixture both DMSO-d_6 and MeOH-d_4 are present and could coordinate to palladium as neutral ligands. A comparison of the ^{1}H NMR spectra for the (η^3-allyl)palladium complexes synthesized in MeOH-d_4, DMSO-d_6, and a 1:1 MeOH-d_4/DMSO-d_6 mixture reveals significant differences.

In MeOH-d_4 solution, all four allylic protons give rise to sharp peaks. However, in both DMSO-d_6 and 1:1 DMSO-d_6/MeOH-d_4 solution the two terminal protons give rise to a single broad peak at room temperature (Figure 6), suggesting a fast η^3−η^1−η^3 exchange is taking place.[17] That this phenomenon is not observed in MeOH-d_4 suggests that the η^3−η^1−η^3 isomerization is induced by DMSO-d_6, and accordingly, this solvent molecule is coordinated to palladium at least to some extent. During the course of the model silylation reaction

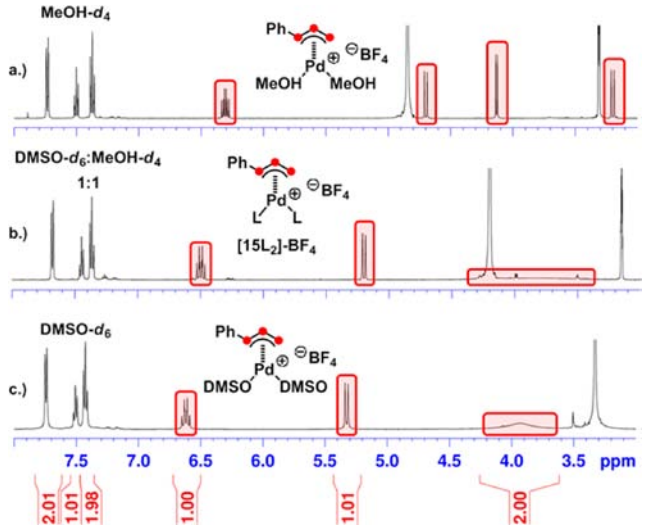

Figure 6. ^{1}H NMR spectra of [**15**L$_2$]−BF$_4$ in different solvents.

(Scheme 3), [Pd(MeCN)$_4$](BF$_4$)$_2$ was found to convert quickly and quantitatively to the new cationic (η^3-allyl) palladium complex. To examine if this complex corresponds to the catalyst resting state, we wanted to determine whether [**15**L$_2$]−BF$_4$ was catalytically competent. We selected acetonitrile complex [**15**(MeCN)$_2$]−BF$_4$ for this study because of its higher stability in the solid state compared to the corresponding DMSO complex [**15**(DMSO)$_2$]−BF$_4$. Performing our model reaction with 5 mol % [**15**(MeCN)$_2$]−BF$_4$ instead of [Pd(MeCN)$_4$](BF$_4$)$_2$ produced **4a** in 73% yield, showing that the complex is catalytically active (Scheme 12). However, in this reaction the presynthesized complex [**15**(MeCN)$_2$]−BF$_4$ was observed to decompose slightly faster than the (η^3-allyl)palladium species formed in situ from [Pd(MeCN)$_4$](BF$_4$)$_2$ under our initial conditions (Scheme

dx.doi.org/10.1021/ja309860h | J. Am. Chem. Soc. 2013, 135, 443−455

Scheme 12. Silylation of 1a Using [15(MeCN)$_2$]−BF$_4$ as a Catalyst[a]

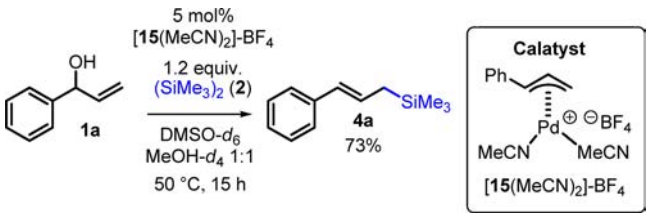

[a]The yield is determined by ^{1}H NMR spectroscopy using an internal standard.

3). In the crude reaction mixture after 15 h with [**15**(MeCN)$_2$]−BF$_4$ as a catalyst, 24% of the linear ether intermediate **12a**-d_3 remained, while all of the (η^3-allyl) palladium catalyst was decomposed.

A possible difference between the reactions catalyzed by [**15**(MeCN)$_2$]−BF$_4$ and [Pd(MeCN)$_4$](BF$_4$)$_2$ is that, in the latter case, BF$_3$ is formed early in the reaction, probably to a large extent during catalyst activation. Addition of 10 mol % of BF$_3$·OEt$_2$ to the reaction catalyzed by [**15**(MeCN)$_2$]−BF$_4$ substantially improved the longevity of the (η^3-allyl)palladium species and raised the NMR yield of **4a** to 91% (Scheme 13).

Scheme 13. Silylation of 1a Using [15(MeCN)$_2$]−BF$_4$ and BF$_3$·OEt$_2$ as Catalysts[a]

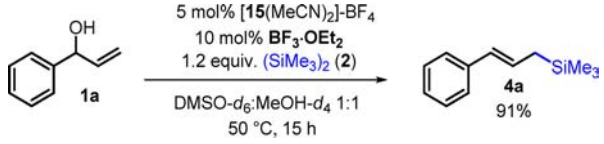

[a]The yield is determined by ^{1}H NMR spectroscopy using an internal standard.

The ^{1}H NMR spectrum of the crude reaction mixture showed that 50% of the added (η^3-allyl)palladium complex was still intact after complete consumption of **1a**. Since catalyst decomposition likely occurs by aggregation of Pd(0) leading to the formation of Pd black, a possible explanation is that BF$_3$ stabilizes the Pd(0) intermediates (see discussion below in section "Formation of Allylic Silane from the (η^3-Allyl) palladium Complexes"). Furthermore, BF$_3$ could activate the alcohol and thereby accelerate the oxidative addition which would lead to a decrease in the concentration of unstable Pd(0) intermediates.

Formation of the Active Catalyst. Having identified the rapid room-temperature formation of catalytically competent complex [**15**L$_2$]−X in our model reaction (Scheme 3), we sought to investigate the conditions under which it is formed. Alcohol **1a** was found to be completely inert to the Pd(0) source Pd$_2$(dba)$_3$ at room temperature (Scheme 14a). After one hour no reaction had taken place according to ^{1}H NMR spectroscopy. However, the inclusion of 2 equiv of BF$_3$·OEt$_2$ resulted in full conversion of alcohol **1a** to the (η^3-allyl) palladium complex [**15**L$_2$]−X (Scheme 14b). The reaction was instantaneous, and no other byproducts were observed. This led us to develop a new method for the synthesis of (η^3-allyl) palladium complexes directly from allylic alcohols (see Supporting Information for further details).

Using [Pd(MeCN)$_4$](BF$_4$)$_2$ as the palladium source under the same conditions with or without BF$_3$·OEt$_2$ resulted in

Scheme 14. Stoichiometric Formation of Complex [15L$_2$]−X

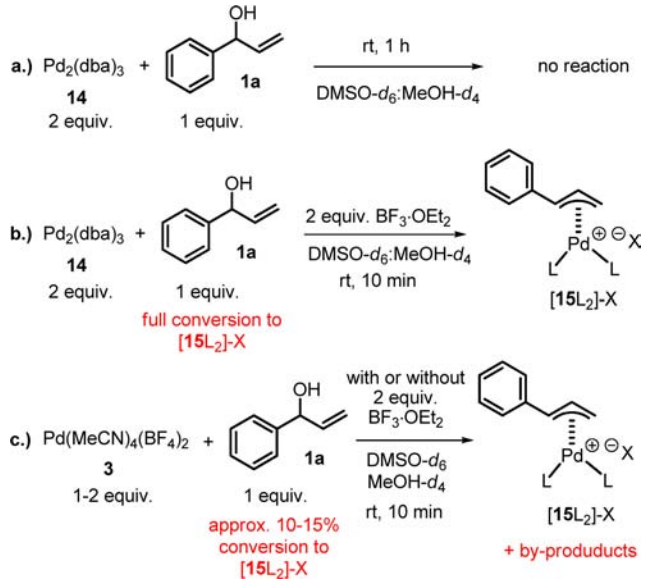

alcohol **1a** being fully consumed within minutes (Scheme 14c). In both reactions (η^3-allyl)palladium complex [**15**L$_2$]−X could be observed to form, however, only as a minor product (approximately 10−15%), and was formed together with a complex mixture of saturated byproducts. Decreasing the amount of [Pd(MeCN)$_4$](BF$_4$)$_2$ in this reaction did not change the outcome significantly, although a small amount of **1a** was still present at the end. That Pd(0) reacts cleanly with **1a**, in the presence of a Lewis acid to form [**15**L$_2$]−X, whereas the corresponding reaction with [Pd(MeCN)$_4$](BF$_4$)$_2$ (**3**) is sluggish suggests that reduction to Pd(0) is key to catalyst activation.

Oxidation of **1a** was not observed during the course of our model reaction (Scheme 3). Similarly, reduction of **3** to palladium black was not observed upon heating at 50 °C in DMSO-d_6/MeOH-d_4 for 15 h. This suggests **1a** and MeOH-d_4 do not behave as reductants for palladium under the applied catalytic conditions. However, the fast formation of Me$_3$Si−F (**7**, Figure 1) and BF$_3$ (**11**) indicates that (Me$_3$Si)$_2$ (**2**) is involved in the reduction of Pd(II) to Pd(0). Heating the Pd(II) salt **3** with (SiMe$_3$)$_2$ (**2**) in the reaction solvent produced a dark red solution in which Me$_3$Si−F and BF$_3$ were detected by ^{19}F and ^{11}B NMR spectroscopy (Scheme 15). After 2 h, palladium black was observed to form. However, if alcohol **1a** was added after 1.5 h this led to the instant formation of the (η^3-allyl)palladium complex [**15**L$_2$]−X, and the solution returned to a yellow color.

Formation of Allylic Silane from (η^3-Allyl)palladium Complexes. After establishing that (η^3-allyl)palladium com-

Scheme 15. Formation of [15L$_2$]−X by in Situ Generation of Pd(0)

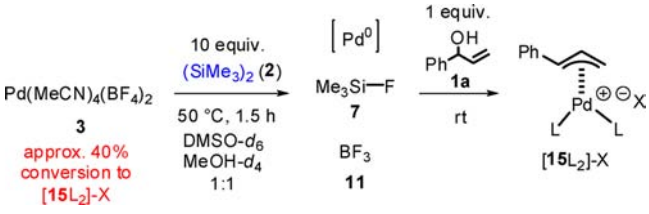

dx.doi.org/10.1021/ja309860h | J. Am. Chem. Soc. 2013, 135, 443−455

plex [**15**L_2]−X is formed in our model reaction (Scheme 3), we investigated its reactivity with $(SiMe_3)_2$ (**2**). A stoichiometric reaction[18] between [**15**$(MeCN)_2$]−BF_4 and $(SiMe_3)_2$ (24 equiv to approximate the catalytic conditions) in DMSO-d_6/MeOH-d_4 (1:1) at 50 °C was monitored by ^{1}H NMR spectroscopy (Scheme 16a). After 10 min a product ratio of

Scheme 16. Stoichiometric Reactions between [15(MeCN)$_2$]−BF$_4$ and 2

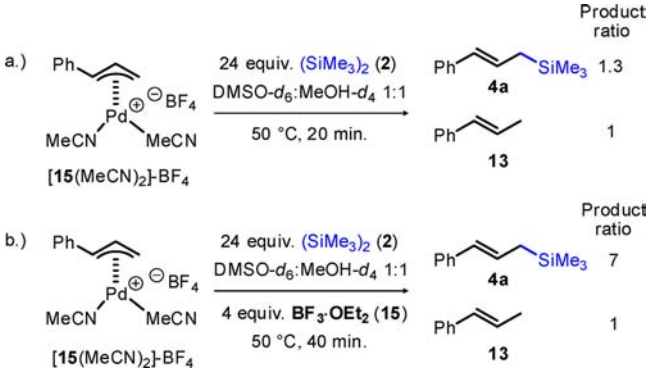

4a:**13** of 7:1 was observed, which decreased to 1.3:1 at full consumption of [**15**$(MeCN)_2$]−BF_4 (20 min). Continued heating did not alter the product ratio, suggesting that **13** is not formed by protodesilylation of **4a**.

The sequential synthesis of **4a** via allylic ethers **12a**-d_3 and **12b**-d_3 (Scheme 6) indicates that the presence of Pd(0) promotes the formation of **13**, which occurs mainly at the end of the stoichiometric reaction (Scheme 16a). Additionally, **13** is formed in approximately 2% NMR yield in the catalytic model reaction (Scheme 3). In the catalytic process (Scheme 3), the concentration of Pd(0) is low for the greater part of the process due to a fast alcohol activation. Increasing the catalyst loading in the model silylation reaction (Scheme 3) also increased the formation of **13** (see Supporting Information, page S6). This result indicates that *trans*-*β*-methylstyrene (**13**) is formed at the end of the reaction as the catalyst starts decomposing. The inclusion of BF_3·OEt_2 in the stoichiometric reaction (Scheme 16b) gave a higher **4a**:**13** ratio of 7:1 but required a longer reaction time (40 min) to achieve complete conversion. A possible explanation for the reduced formation of *trans*-*β*-methylstyrene (**13**) is that BF_3 coordinates to Pd(0) as a so-called "Z-type ligand" (*σ*-acceptor ligand).[19] This is consistent with our observation that a substantial amount of homogeneous Pd(0) can be present in a BF_3-containing DMSO-d_6/MeOH-d_4 solution at 50 °C without palladium black formation being observed (Scheme 15).

Formation of Me_3Si−F (**7**) in the stoichiometic reaction shown in Scheme 16a demonstrates that the BF_4^- counterion of [**15**$(MeCN)_2$]−BF_4 takes part in the reaction. We propose that BF_4^- helps in the activation of $(SiMe_3)_2$ (**2**) toward transmetalation to give Me_3Si−F (**7**) and a palladium complex with a trimethylsilyl ligand (Scheme 17). This likely mimics the transmetalation step in the first cycle of the catalytic reaction (Scheme 3). Additionally, that silyl-Pd species were not observed is consistent with a fast reductive elimination in which **4a** is formed.

The stoichiometric reaction between complex [**15**$(MeCN)_2$]−BF_4 and $(SiMe_3)_2$ at 25 °C afforded both **12a**-d_3 and **4a** (3:1 ratio, see Supporting Information for more

Scheme 17. Allylic Silane 4a and 7 Were the Only Silicon-Containing Products Observed to Form in the Reaction Depicted In Scheme 16a

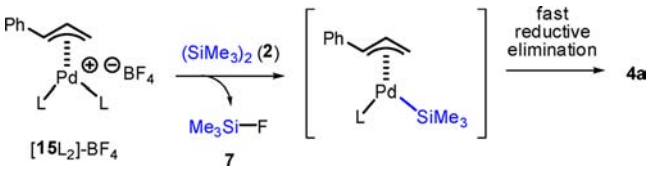

information). This indicates that the formation of **12a**-d_3 via (η^3-allyl)palladium intermediates is possible under our catalytic conditions but that higher temperatures favor the formation of **4a**.

Relative Concentration of the Reaction Components as a Function of Time. The key reaction components of our model system (Scheme 3) were monitored by ^{1}H NMR spectroscopy for 12 h (Figure 7). The (η^3-allyl)palladium

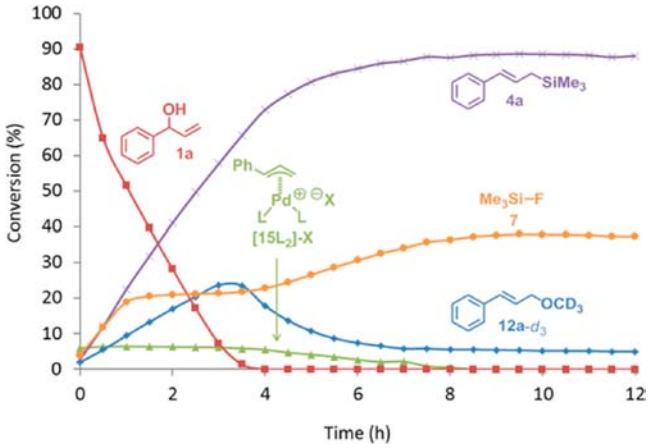

Figure 7. Overview of the reaction components over time. The conversion refers to the silylation of **1a** in formation of **4a**. Lines are given as a guide for the eye.

complex [**15**L_2]−X is formed quickly at the start of the reaction and remains at a constant concentration (approximately 5 mol %) until **1a** is consumed completely. As shown previously, allylic ether **12a**-d_3 forms at the start, and it reaches its maximum concentration after 3.5 h, coinciding with the alcohol being consumed. Me_3Si−F (**7**) is formed at the same rate as the product for the first hour, and the rate of its formation is thereafter reduced. When the reaction is finished, its maximum theoretical conversion of 40% has almost been reached (using all available fluorides from a 10 mol % loading of BF_4^-).

Kinetic Studies: Reagent Order Determination. Initial rate measurements were carried out to identify the turnover limiting step. The initial rate dependence on the concentration of hexamethyldisilane (**2**) (Figure 8a), [$Pd(MeCN)_4$](BF_4)$_2$ (**3**) (Figure 8b), alcohols **1a** and **1b** (Figure 8c,d), and methanol (Figure 8e) was evaluated.

The reaction was observed as approximately first order in hexamethyldisilane and [$Pd(MeCN)_4$](BF_4)$_2$ but zero order in isomeric allylic alcohols **1a**,**b**. Varying the concentration of methanol had a drastic effect on the rate. The reaction showed third-order dependence in methanol in the range of [MeOH-d_4] = 15.5−18.6 M. Our kinetic studies, combined with the identification of the (η^3-allyl)palladium complex [**15**L_2]−X as a key intermediate and the catalyst resting state, are consistent

dx.doi.org/10.1021/ja309860h | J. Am. Chem. Soc. 2013, 135, 443−455

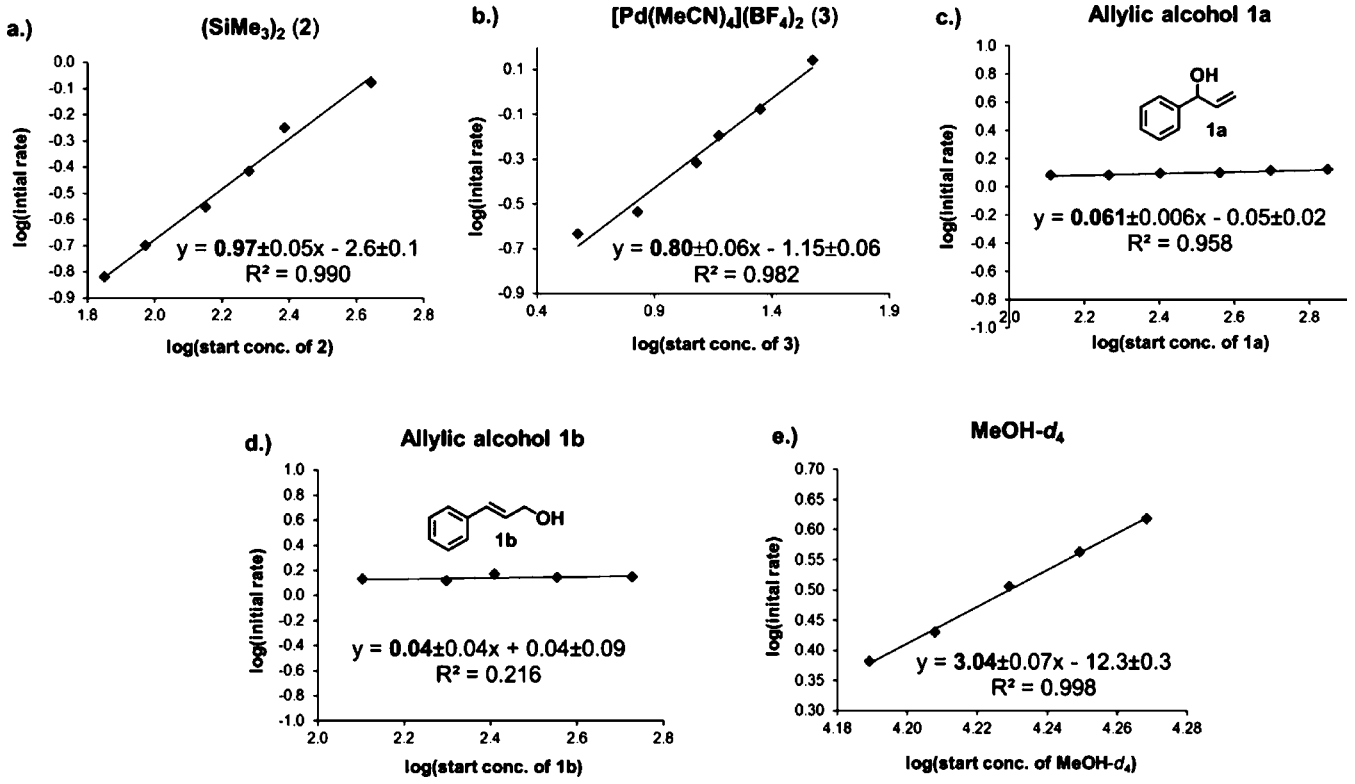

Figure 8. Dependence of the logarithm of the initial rate on the logarithm of the concentration of (a) $(SiMe_3)_2$, (b) $[Pd(MeCN)_4](BF_4)_2$, (c) allylic alcohol **1a**, (d) allylic alcohol **1b**, and (e) MeOH-d_4.

with the following conclusions about the mechanism of the model silylation process:

- C−OH cleavage is not turnover limiting.
- Complex $[\mathbf{15}L_2]$−X, which is rapidly formed from $[Pd(MeCN)_4](BF_4)_2$, participates in the turnover limiting step.
- The turnover limiting step involves $(SiMe_3)_2$ (**2**).

The silylation (and borylation) of allylic alcohols proceeds rapidly when methanol is used as solvent or cosolvent.[2a,b,8] The use of both DMSO-d_6 and MeOH-d_4 as solvents in the studied catalytic silylation was crucial to obtain a fast and clean reaction.[2a] In pure DMSO-d_6, the conversion of **1** to **4** is very slow, and if the reaction is performed in pure methanol byproduct formation becomes a problem.[2a] The rate dependence observed for methanol concentration is interesting from a practical synthetic perspective but somewhat difficult to rationalize. Unfortunately, the poor solubility of $(SiMe_3)_2$ in DMSO-d_6 prevented the study of the rate dependence in a wider MeOH-d_4 concentration range. It seems that MeOH-d_4 is needed both to dissolve $(SiMe_3)_2$ as well as to facilitate the turnover limiting step of the reaction. A possible explanation for the third-order dependence on methanol is organization of three methanol molecules by hydrogen bonding in the rate-determining step. Sigman and co-workers[20] reported a similar third-order dependence of water in the Wacker oxidation, proposing the preorganization of three water molecules in the rate-determining step. We performed a solvent isotope effect experiment to further investigate the role of MeOH in our reaction. However, we observed no appreciable difference in rate between the reactions performed in CD_3OH and those performed in CD_3OD (see pages S12−13, Supporting Information).

Mechanism of the Borylation Reaction. To investigate the similarities between the borylation and the silylation reactions (Scheme 2), the analogous borylation of **1a** using bis(pinacolato)diboron (**5**) was chosen as a model reaction (Scheme 18).

Scheme 18. Model Reaction for Studying the Borylation[a]

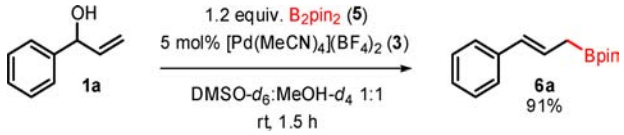

[a]The yield is determined by ^{1}H NMR spectroscopy using an internal standard.

Following the course of the reaction by ^{19}F NMR spectroscopy revealed a more gradual formation of BF_3 compared to the silylation process. Additionally, a peak corresponding to BF_3OH^- was identified[21] by comparison with previously reported shift values (Figure 9). The crude reaction mixture was also studied using ^{11}B NMR spectroscopy. The product (**6a**) and the excess B_2pin_2 (pin = pinacolato) gave rise to two partially overlapping peaks at 32 and 30 ppm (Figure 10). The only byproduct observed containing a Bpin adduct is pinB−OH (**16**).[22] Analogously to the silylation reaction, $B(OR)_3$ (R = H or CD_3) is also formed, but in larger amounts; $B(OR)_3$ is formed mainly via hydrolysis of pinB−OH and not only from the catalyst counterion BF_4^-.

Unlike for the silylation reaction, which is accompanied with formation of Me_3Si−F (**7**), pinB−F (**17**)[23] is not observed accompanying the formation of BF_3 in the borylation. It is possible that pinB−F is initially formed and thereafter

dx.doi.org/10.1021/ja309860h | J. Am. Chem. Soc. 2013, 135, 443−455

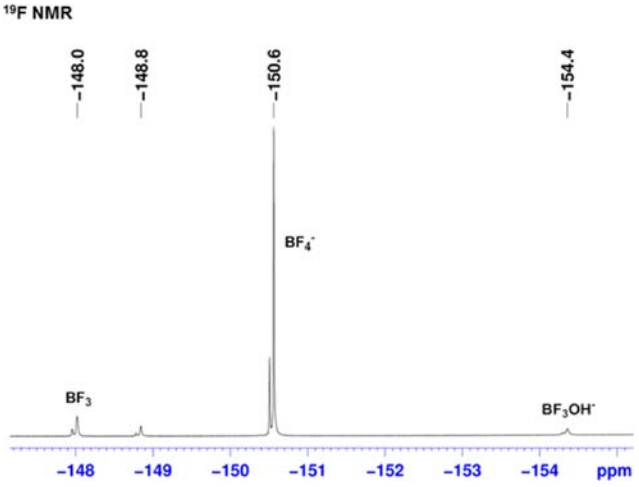

Figure 9. ^{19}F NMR spectrum of the crude reaction mixture after complete conversion of **1a** to **6a** (Scheme 18).

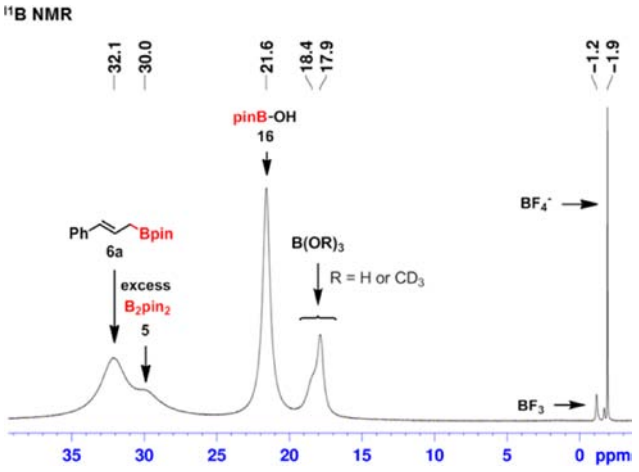

Figure 10. ^{11}B NMR spectrum of the crude reaction mixture after complete conversion of **1a** to **6a** (Scheme 18).

hydrolyzed to $B(OR)_3$ (R = H or CD_3), which was shown to form. Monitoring the model borylation reaction (Scheme 18) by ^{1}H NMR spectroscopy (Figure 11) revealed the presence of

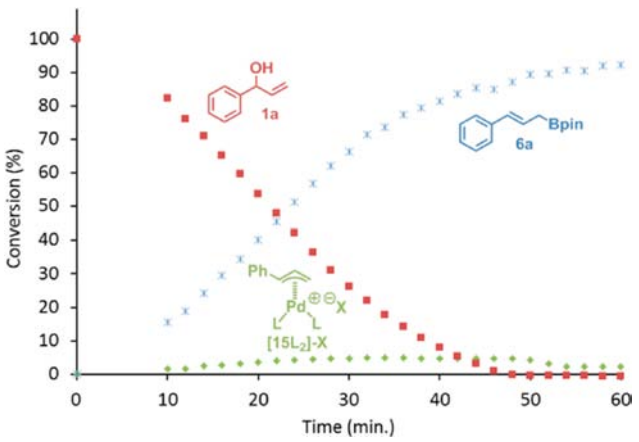

Figure 11. Overview of the reaction components of the borylation over time. The conversion refers to the borylation of **1a** in formation of **6a**.

the same (η^3-allyl)palladium intermediate ([**15**L_2]−X) observed in the corresponding silylation. It took 30 min for [**15**L_2]−X to reach its maximum concentration (5 mol %) which was maintained until the allylic alcohol (**1a**) was fully consumed. Allylic ethers **12a**-d_3 and **12b**-d_3 were not observed in this reaction.

Using (η^3-allyl)palladium complex [**15**$(MeCN)_2$]−BF_4 as a catalyst in the borylation with the addition of $BF_3{\cdot}OEt_2$ resulted in a 98% NMR yield of **6a** (Scheme 19), demonstrating its

Scheme 19. Borylation of 1a Using [15(MeCN)$_2$]−BF$_4$ and BF$_3$·OEt$_2$ as Catalysts[a]

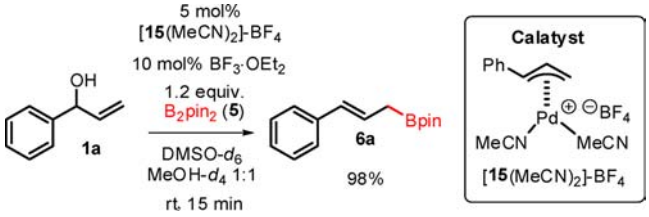

[a]The yield is determined by ^{1}H NMR spectroscopy using an internal standard.

catalytic competence in analogy with the silylation reaction (cf. Scheme 13). Additionally, the stoichiometric reaction between (η^3-allyl)palladium complex [**15**$(MeCN)_2$]−BF_4 and B_2pin_2 gave clean conversion to **6a** (Scheme 20). These results strongly suggest that [**15**L_2]−X is the catalyst resting state, in analogy with the silylation reaction discussed above.

Scheme 20. Stoichiometric Reaction between [15(MeCN)$_2$]−BF$_4$ and 5

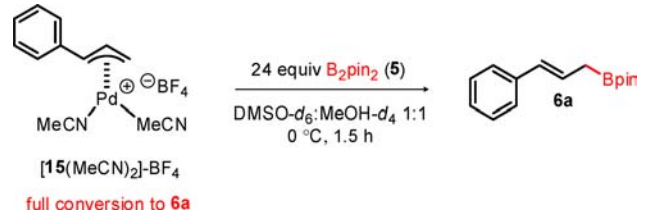

In summary, in both the silylation and the borylation the strong Lewis acid BF_3 is formed and likely promotes C−OH cleavage. In both reactions the (η^3-allyl)palladium complex [**15**L_2]−X is formed, which acts as an active catalyst. Both the silylation and the borylation involve a transmetalation-reductive elimination sequence of the (η^3-allyl)palladium intermediate to give allylic silane or allylic boronate products.

Stereoselectivity of the Reaction. The high stereoselectivity of the reactions is an important synthetic advantage. Moreover, the stereochemical outcome of the reaction can reveal important mechanistic details. Both the formation of the (η^3-allyl)palladium intermediate and the nature of the reductive elimination in these reactions will influence the configuration of the final products.

Using conditions we previously reported for the stereoselective silylation of allylic alcohols, *cis*-**1c** afforded **4b** in 52% isolated yield (3:1 *trans*:*cis* mixture).[2a] The analogous borylation proceeded more cleanly and with higher stereoselectivity, giving **6b** in 70% isolated yield and a *trans*:*cis* ratio of 5:1 (Scheme 21). The silylation of *cis*-**1c** is difficult to monitor by ^{1}H NMR spectroscopy. Therefore, considering the close

dx.doi.org/10.1021/ja309860h | J. Am. Chem. Soc. 2013, 135, 443−455

Scheme 21. Silylation[a] and Borylation[b]

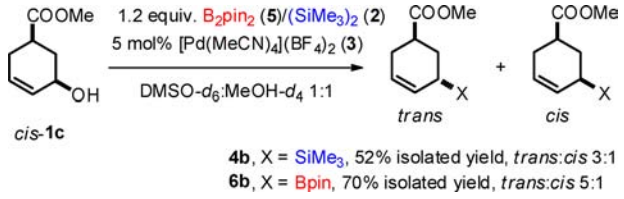

[a]The reaction was stirred at 60 °C for 15 h. [b]The reaction was stirred at 20 °C for 1.5 h.

similarity in the reaction mechanisms, the borylation of *cis*-**1c** was chosen as a model reaction to investigate the stereoselectivity (Scheme 21). The reaction was initially monitored by ^{1}H NMR spectroscopy. The loading of $[Pd(MeCN)_4](BF_4)_2$ was increased to 10 mol % to make observation of the catalyst more accurate. Both complexes *cis*-[**18**L_2]−X and *trans*-[**18**L_2]−X formed during the reaction (Figure 12),[13] reaching

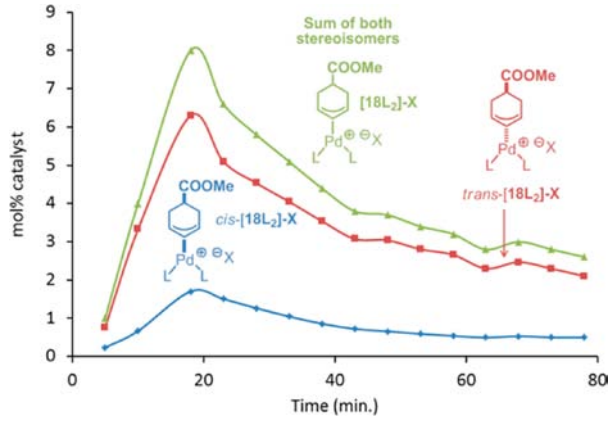

Figure 12. Borylation of *cis*-**1c** was followed by ^{1}H NMR spectroscopy under standard borylation conditions (see Scheme 21) with the exception that 10 mol % of **3** was used. Lines are given as a guide for the eye.

their maximum concentration after 20 min (8 mol % total) and decreasing thereafter. The *trans* complex was shown to be the major stereoisomer formed, likely via oxidative addition with inversion from *cis*-**1c**, in accordance with previous studies.[24] Also, allyl boronate product *trans*-**6b** was observed to form at a much higher rate than *cis*-**6b** throughout the reaction (Figure 13).

These findings make it reasonable to assume that boronate *trans*-**6b** forms from complex *trans*-[**18**L_2]−X and *cis*-**6b** from *cis*-[**18**L_2]−X via reductive elimination with retention of configuration. As the *trans*-**6b**:*cis*-**6b** ratio is consistently higher than the *trans*-[**18**L_2]−X:*cis*-[**18**L_2]−X, the (η^3-allyl)palladium complex *trans*-[**18**L_2]−X likely undergoes much faster turnover than *cis*-[**18**L_2]−X does.

We also studied (by ^{1}H NMR spectroscopy) the stoichiometric reaction between complex *trans*-[**18**$(MeCN)_2$]−BF_4 and B_2pin_2 at room temperature. A 1:1 mixture of *trans*-**6b** and *cis*-**6b** was formed in a single step (Scheme 22) with no observed intermediates, which is indicative of a fast reductive elimination, in keeping with our previous findings. However, the scrambling of the stereochemistry is in contradiction with the results from the catalytic reaction (Scheme 21 and Figure 13).

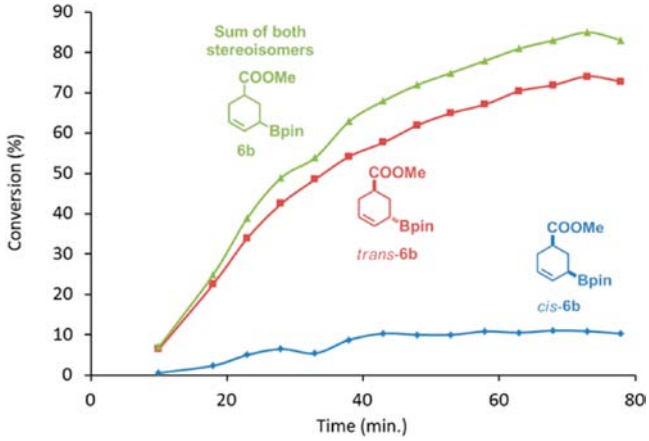

Figure 13. Borylation of **1c** was followed by ^{1}H NMR spectroscopy under standard borylation conditions (see Scheme 21) with the exception that 10 mol % of **3** was used. The conversion refers to the borylation of **1c** in formation of **6b**. Lines are given as a guide for the eye.

Scheme 22. Stoichiometric Reactions between *trans*-[18$(MeCN)_2$]−BF_4 and 5

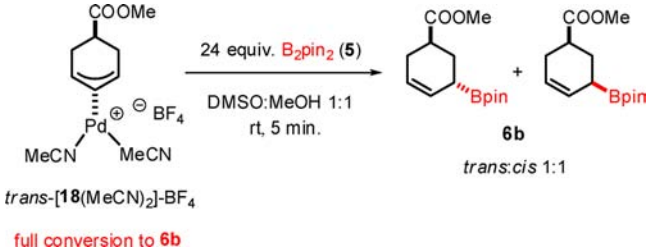

A possible explanation is that Pd(0) formed by the reductive elimination epimerizes complex *trans*-[**18**$(MeCN)_2$]−BF_4 to give a mixture of *trans*- and *cis*-[**18**$(MeCN)_2$]−BF_4. Bäckvall and co-workers have proposed that *cis*−*trans* isomerization in related (η^3-allyl)palladium complexes can result from nucleophilic attack by free Pd(0) on the (η^3-allyl)palladium complex.[24b] We therefore reasoned that the lack of stereoselectivity in our stoichiometric reaction (Scheme 22) similarly may be explained by the high relative concentration of Pd(0), which forms via reductive elimination.

To further investigate the effects of Pd(0) on the stereochemical outcome of the reaction, 5 mol % of $Pd_2(dba)_3$ was added to the borylation of *cis*-**1c** under our standard catalytic conditions (Figure 14). The reaction produced **6b** in substantially lower NMR yield and lower (3:1) *trans*:*cis* selectivity, showing that Pd(0) has an adverse effect on the stereochemistry of the reaction. This suggests that the *cis*−*trans* isomerization should be suppressed by lowering the concentration of free Pd(0). Indeed, the addition of 30 mol % of $BF_3{\cdot}OEt_2$ to the borylation reaction increased the *trans*-**6b**:*cis*-**6b** ratio as well as the NMR yield (Figure 14). We reasoned that addition of $BF_3{\cdot}OEt_2$ accelerated the oxidative addition of Pd(0) to the allylic alcohol substrate. Therefore, the concentration of free Pd(0) decreased, leading to less isomerization and, therefore, higher stereoselectivity. In addition, a reduction in catalyst loading (2.5 mol %) further improved the stereoselectivity to *trans*:*cis* 11:1 (Figure 14). This can be explained by the fact that two palladium atoms are involved in the Pd(0)-catalyzed isomerization.[24b] Thus, a

dx.doi.org/10.1021/ja309860h | J. Am. Chem. Soc. 2013, 135, 443−455

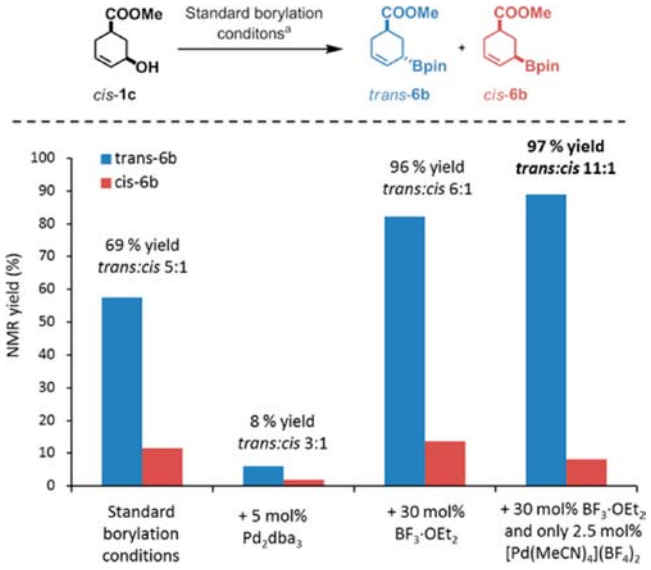

Figure 14. Investigation into the effects of additives on the stereoselectivity of the borylation. [a]Standard borylation conditions: **5** (1.2 equiv), **3** (5 mol %), DMSO-d_6/MeOH-d_4 1:1, rt, 1.5 h. The yields are determined by ^{1}H NMR spectroscopy using an internal standard.

decrease in the total concentration of palladium discourages isomerization and favors transmetalation instead.

Proposed Catalytic Cycle. On the basis of the above mechanistic studies, we propose a catalytic cycle in Figure 15. The major initiation pathway is proposed to proceed via complex **3** undergoing two consecutive transmetalations with $(SiMe_3)_2$ (**2**) in which Me_3Si-F and BF_3 are formed (Figure 15). Reductive elimination will then regenerate 1 equiv of $(SiMe_3)_2$ with respect to the catalyst and a Pd(0) complex with loosely coordinated ligands. Thereafter $[\mathbf{15}L_2]-X$ is proposed to form by oxidative addition of the alcohol to Pd(0). The activation of the allylic alcohol by BF_3 to form free allyl cations prior to the reaction with Pd(0) cannot be excluded.[25] However, due to the fast formation of $[\mathbf{15}L_2]-X$, a direct oxidative addition to the activated alcohol is considered a more likely reaction pathway. Our stoichiometric studies show that formation of the (η^3-allyl)palladium complex $[\mathbf{15}L_2]-X$ only occurs if the hydroxyl group is activated, for example, by BF_3 (Scheme 15). Under catalytic conditions BF_3 (**11**) is formed from the counterion of $[Pd(MeCN)_4](BF_4)_2$ (**3**). Alternatively, the cationic Pd(II) complex $[\mathbf{15}L_2]-X$ could act as a Lewis acid.[26] However, the fact that the hydroxyl group is transferred to boron rather than silicon at the start of the reaction supports the assumption that BF_3 or its derivatives are coordinated to the alcohol in the C–O bond-breaking step.

Our study of the stereochemistry of the borylation indicates that the formation of (η^3-allyl)palladium species by oxidative addition is stereoselective and occurs with inversion. As both the borylation and the silylation proceed via (η^3-allyl)palladium species, it is reasonable to assume that the oxidative addition during the silylation occurs with the same stereochemistry. Thereafter, the formed complex probably undergoes Pd(0)-catalyzed isomerization (Figures 12–14, Schemes 21–22). This is in accordance with the lower stereoselectivity observed for the silylation compared to the borylation (Scheme 21); the former has a longer reaction time and therefore a greater opportunity for the (η^3-allyl)palladium complex to isomerize.

It has been shown that allylic ether **12a**-d_3 can form both from the reaction of the (η^3-allyl)palladium complex $[\mathbf{15}(MeCN)_2]-BF_4$ with methanol (Supporting Information) and without the assistance of palladium complexes from alcohol **1a** by BF_3-catalyzed nucleophilic substitution (Scheme 10). In the Pd-catalyzed reaction, mainly linear ether **12a**-d_3 and only trace amounts of branched ether **12b**-d_3 are formed (Schemes 5 and 6). By contrast, in the BF_3-catalyzed process (in the absence of Pd) formation of the branched ether **12b**-d_3 is preferred over the linear analog **12a**-d_3. This indicates that under catalytic conditions the predominant formation of **12a**-d_3 arises from reaction of $[\mathbf{15}L_2]-X$ with MeOH-d_4. That **12a**-d_3 is both formed and then consumed during the reaction indicates that this process is reversible.

That (η^3-allyl)palladium complex $[\mathbf{15}L_2]-X$ was observed in both the silylation of allylic alcohol **1a** and allylic ether **12a** further suggests that both species are converted by the same

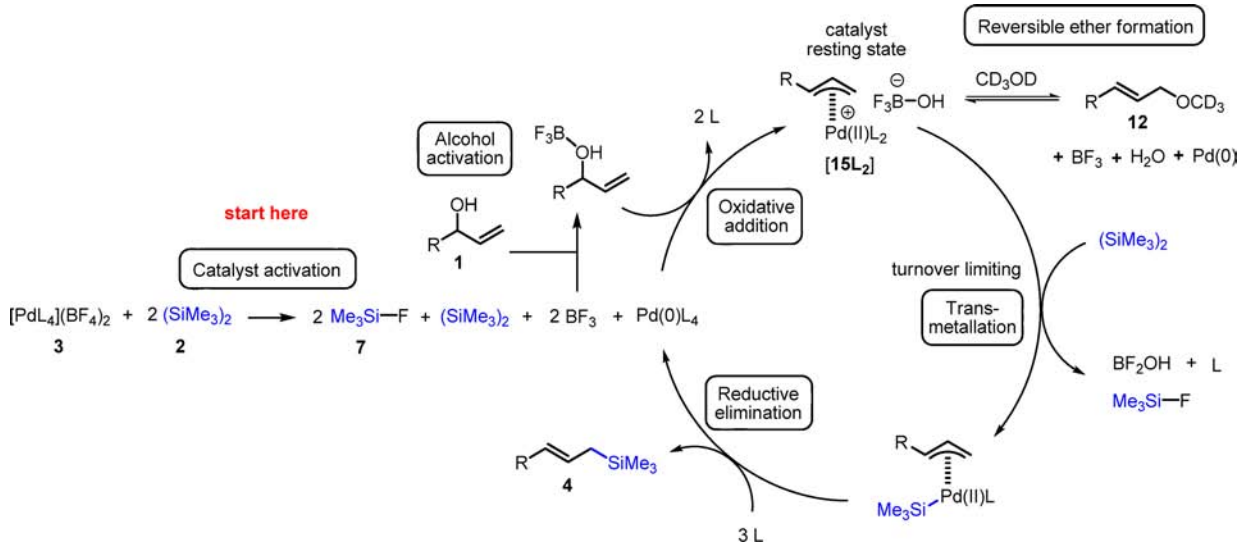

Figure 15. Proposed mechanism of the first turnover of the palladium-catalyzed allylic silylation reaction. The exact nature of the borate species may vary for subsequent turnovers as BF_4^- is converted to $BF_{4-x}X_x$ (X = OH, OCD_3) throughout the catalysis.

dx.doi.org/10.1021/ja309860h | J. Am. Chem. Soc. 2013, 135, 443–455

mechanism into **4a**. According to the competition experiment in Figure 4, alcohol **1a** is converted to **4a** faster than the corresponding ether **12a**, possibly because **1a** is more easily activated by the Lewis acid.

Complex [**15**L_2]−X has also been shown to react with $(SiMe_3)_2$ in formation of **4a** (Scheme 16). The next step in the catalytic cycle is therefore proposed to be transmetalation between the formed (η^3-allyl)palladium complex and $(SiMe_3)_2$. On the basis of the observation that **4a** and Me_3Si−F are the only silicon-containing compounds formed in a stoichiometric reaction between complex [**15**$(MeCN)_2$]−BF_4 and $(SiMe_3)_2$ (Scheme 16a), we propose that the counterion of the palladium complex activates $(SiMe_3)_2$ toward transmetalation. The nature of the counterion varies during the course of the reaction (e.g., BF_4^-, $BF_3OD_3^-$, BF_3OH^-), which is the reason for the formation of compounds Me_3Si−F (**7**), Me_3Si−OCD_3 (**8**), and Me_3Si−OH (**9**) in the catalytic reaction.

The stereochemistry of the process (Figures 12 and 13) indicates that the favored pathway of the catalytic borylation involves the introduction of Bpin via transmetalation to *trans*-[**18**L_2]−X, which forms selectively during oxidative addition. Subsequent reductive elimination produces *trans*-**6b** (Figure 13), which is consistent with the *trans*-**4b** product forming analogously as the major isomer in the silylation (Scheme 21).

Our kinetic studies show a rate dependence on both the palladium precursor **3** and $(SiMe_3)_2$ (**2**) in the silylation. Monitoring of this reaction by ^1H NMR clearly shows that quantitative formation of complex [**15**L_2]−X is fast. We therefore propose that transmetalation of [**15**L_2]−X with $(SiMe_3)_2$ (**2**) is the turnover limiting step. The fast formation of [**15**L_2]−X, its presence at a steady 5 mol % (the theoretical maximum), as well as its catalytic competence indicate that it is the catalyst resting state. This is also in agreement with the zero-order kinetics for alcohol **1a** since increasing the concentration of **1a** will not influence the concentration of complex [**15**L_2]−X.

CONCLUSIONS

On the basis of the above studies, the most important mechanistic aspects of the synthetically useful silylation and borylation of allylic alcohols are now well understood:

- It has been shown that BF_3 is formed from the BF_4^- counterion of catalyst **3** during the silylation and that a catalytic amount of this Lewis acid is able to efficiently activate the hydroxyl group under our catalytic conditions.
- The key intermediate of the silylation reaction is an (η^3-allyl)palladium complex formed by oxidative addition to the activated allylic alcohol substrate. The (η^3-allyl)palladium complex is also the resting state of the catalyst.
- The turnover limiting step of the silylation is transmetalation of $(SiMe_3)_2$ with the (η^3-allyl)palladium complex. This step proceeds with a high stereoselectivity, in particular for the borylation process. Interestingly, cleavage of the C−OH group is not rate limiting.
- The silylation and borylation proceed according to very similar mechanisms. In both reactions BF_3 is formed and is able to activate the alcohol substrate. Both reactions proceed via (η^3-allyl)palladium intermediates.

Our insights into the mechanism have also allowed a substantial improvement in the stereoselectivity of the palladium-catalyzed borylation of allylic alcohols by increasing the rate of oxidative addition and lowering the catalyst loading. Additionally, we have shown that (η^3-allyl)palladium complexes can be prepared conveniently directly from allylic alcohols. The above mechanistic study will certainly open new synthetic routes for the application of allylic alcohols in selective organic synthesis and open new opportunities for easy access to stereo- and regiodefined allylic silanes and allylic boronates, which are very important reagents in advanced organic synthesis.[4,27]

EXPERIMENTAL DETAILS

Model Silylation Reaction. The corresponding allylic alcohol **1a** (0.15 mmol) and **2** (0.18 mmol) were added to a solution of DMSO-d_6 and MeOH-d_4 (0.2 mL/0.2 mL) containing palladium precatalyst **3** (0.0075 mmol, 5 mol %). Thereafter, the reaction mixture was stirred at 50 °C for 15 h.

Model Borylation Reaction. The corresponding allylic alcohol **1a** (0.15 mmol) was added to a solution of **5** (0.18 mmol) and palladium precatalyst **3** (0.0075 mmol, 5 mol %) in DMSO-d_6 and MeOH-d_4 (0.2 mL/0.2 mL). Thereafter, the reaction mixture was stirred at room temperature for 1.5 h.

ASSOCIATED CONTENT

Supporting Information

Experimental procedures and spectroscopic and kinetic data. This material is available free of charge via the Internet at http://pubs.acs.org.

AUTHOR INFORMATION

Corresponding Author

kalman@organ.su.se

Notes

The authors declare no competing financial interest.

ACKNOWLEDGMENTS

The authors thank the financial support of the Swedish Research Council (VR) and the Knut och Alice Wallenbergs Foundation. We thank Dr. Lukasz T. Pilarski, Department of Chemistry-BMC, Uppsala University, for help with the synthesis of complex **18**-Cl and Rauful Alam, Department of Organic Chemistry, Stockholm University, for help with the synthesis of **14**.

REFERENCES

(1) (a) Sundararaju, B.; Achard, M.; Bruneau, C. *Chem. Soc. Rev.* **2012**, *41*, 4467−83. (b) Tamaru, Y. *Eur. J. Org. Chem.* **2005**, 2647−56. (c) Muzart, J. *Tetrahedron* **2005**, *61*, 4179−212. (d) Szabó, K. J. *Synlett* **2006**, *2006*, 811−24. (e) Bandini, M. *Angew. Chem., Int. Ed.* **2011**, *50*, 994−5.

(2) (a) Selander, N.; Paasch, J. R.; Szabó, K. J. *J. Am. Chem. Soc.* **2010**, *133*, 409−11. (b) Olsson, V. J.; Sebelius, S.; Selander, N.; Szabó, K. J. *J. Am. Chem. Soc.* **2006**, *128*, 4588−9. (c) Defieber, C.; Ariger, M. A.; Moriel, P.; Carreira, E. M. *Angew. Chem., Int. Ed.* **2007**, *46*, 3139−43. (d) Mukherjee, P.; Widenhoefer, R. A. *Org. Lett.* **2010**, *12*, 1184−7. (e) Kimura, M.; Futamata, M.; Mukai, R.; Tamaru, Y. *J. Am. Chem. Soc.* **2005**, *127*, 4592−3. (f) Ozawa, F.; Okamoto, H.; Kawagishi, S.; Yamamoto, S.; Minami, T.; Yoshifuji, M. *J. Am. Chem. Soc.* **2002**, *124*, 10968−9.

(3) (a) Youngsaye, W.; Lowe, J. T.; Pohlki, F.; Ralifo, P.; Panek, J. S. *Angew. Chem., Int. Ed.* **2007**, *46*, 9211−4. (b) Kong, K.; Moussa, Z.; Lee, C.; Romo, D. *J. Am. Chem. Soc.* **2011**, *133*, 19844−56. (c) Donohoe, T. J.; Winship, P. C. M.; Tatton, M. R.; Szeto, P. *Angew. Chem., Int. Ed.* **2011**, *50*, 7604−6. (d) Wohlfahrt, M.; Harms, K.; Koert, U. *Angew. Chem., Int. Ed.* **2011**, *50*, 8404−6. (e) Trost, B. M.; Dong, G. *Nature* **2008**, *456*, 485−8. (f) Wan, S.; Wu, F.; Rech, J. C.; Green, M. E.; Balachandran, R.; Horne, W. S.; Day, B. W.; Floreancig, P. E. *J. Am. Chem. Soc.* **2011**, *133*, 16668−79. (g) Langkopf, E.; Schinzer, D. *Chem. Rev.* **1995**, *95*, 1375−408. (h) Hall, D. G., Ed.

Boronic Acids: Preparation and Applications in Organic Synthesis, Medicine and Materials, 2nd ed.; Wiley-VCH Verlag GmbH & Co. KGaA: New York, 2011.
(4) (a) Masse, C. E.; Panek, J. S. *Chem. Rev.* **1995**, *95*, 1293−316. (b) Fleming, I.; Barbero, A.; Walter, D. *Chem. Rev.* **1997**, *97*, 2063−192. (c) Hall, D. G. *Pure Appl. Chem.* **2008**, *80*, 913−27. (d) Kennedy, J. W. J.; Hall, D. G. *Angew. Chem., Int. Ed.* **2003**, *42*, 4732−9. (e) Yamamoto, Y.; Asao, N. *Chem. Rev.* **1993**, *93*, 2207−93. (f) Thibaudeau, S.; Gouverneur, V. *Org. Lett.* **2003**, *5*, 4891−3. (g) Wilkinson, S. C.; Lozano, O.; Schuler, M.; Pacheco, M. C.; Salmon, R.; Gouverneur, V. *Angew. Chem., Int. Ed.* **2009**, *48*, 7083−6. (h) Pilarski, L. T.; Szabo, K. J. *Curr. Org. Chem.* **2011**, *15*, 3389−414.
(5) (a) Sore, H. F.; Galloway, W. R. J. D.; Spring, D. R. *Chem. Soc. Rev.* **2012**, *41*, 1845−66. (b) Miyaura, N.; Suzuki, A. *Chem. Rev.* **1995**, *95*, 2457−83. (c) Denmark, S. E.; Regens, C. S. *Acc. Chem. Res.* **2008**, *41*, 1486−99.
(6) (a) Hatanaka, Y.; Hiyama, T. *J. Org. Chem.* **1988**, *53*, 918−20. (b) Denmark, S. E.; Werner, N. S. *J. Am. Chem. Soc.* **2008**, *130*, 16382−93.
(7) (a) Larsson, J. M.; Zhao, T. S. N.; Szabó, K. J. *Org. Lett.* **2011**, *13*, 1888−91. (b) Ishiyama, T.; Ahiko, T.; Miyaura, N. *Tetrahedron Lett.* **1996**, *37*, 6889−92. (c) Ito, H.; Kawakami, C.; Sawamura, M. *J. Am. Chem. Soc.* **2005**, *127*, 16034−5. (d) Tsuji, Y.; Funato, M.; Ozawa, M.; Ogiyama, H.; Kajita, S.; Kawamura, T. *J. Org. Chem.* **1996**, *61*, 5779−87. (e) Moser, R.; Nishikata, T.; Lipshutz, B. H. *Org. Lett.* **2010**, *12*, 28−31. (f) Hartwig, J. F. *Acc. Chem. Res.* **2011**, *45*, 864−73. (g) Mkhalid, I. A. I.; Barnard, J. H.; Marder, T. B.; Murphy, J. M.; Hartwig, J. F. *Chem. Rev.* **2010**, *110*, 890−931. (h) Hartwig, J. F. *Chem. Soc. Rev.* **2011**, *40*, 1992−2002. (i) Hayashi, T.; Konishi, M.; Ito, H.; Kumada, M. *J. Am. Chem. Soc.* **1982**, *104*, 4962−3. (j) Matsumoto, Y.; Ohno, A.; Hayashi, T. *Organometallics* **1993**, *12*, 4051−5.
(8) Dutheuil, G.; Selander, N.; Szabó, K. J.; Aggarwal, V. K. *Synthesis* **2008**, *2008*, 2293−7.
(9) (a) Selander, N.; Sebelius, S.; Estay, C.; Szabó, K. J. *Eur. J. Org. Chem.* **2006**, *2006*, 4085−7. (b) Selander, N.; Kipke, A.; Sebelius, S.; Szabó, K. J. *J. Am. Chem. Soc.* **2007**, *129*, 13723−31. (c) Aydin, J.; Kumar, K. S.; Sayah, M. J.; Wallner, O. A.; Szabó, K. J. *J. Org. Chem.* **2007**, *72*, 4689−97.
(10) Sebelius, S.; Olsson, V. J.; Wallner, O. A.; Szabó, K. J. *J. Am. Chem. Soc.* **2006**, *128*, 8150−1.
(11) Grubb, W. T. *J. Am. Chem. Soc.* **1954**, *76*, 3408−14.
(12) (a) Bacon, J.; Gillespie, R. J.; Quail, J. W. *Can. J. Chem.* **1963**, *41*, 3063−9. (b) Bacon, J.; Gillespie, R. J.; Hartman, J. S.; Rao, U. R. K. *Mol. Phys.* **1970**, *18*, 561−70.
(13) Identified by comparison with a genuine sample.
(14) (a) Mesmer, R. E.; Palen, K. M.; Baes, C. F. *Inorg. Chem.* **1973**, *12*, 89−95. (b) Lennox, A. J. J.; Lloyd-Jones, G. C. *J. Am. Chem. Soc.* **2012**, *134*, 7431−41.
(15) Kimura, M.; Futamata, M.; Shibata, K.; Tamaru, Y. *Chem. Commun.* **2003**, 234−5.
(16) Murahashi, S.; Imada, Y.; Taniguchi, Y.; Higashiura, S. *J. Org. Chem.* **1993**, *58*, 1538−45.
(17) (a) Solin, N.; Szabó, K. J. *Organometallics* **2001**, *20*, 5464−71. (b) Breutel, C.; Pregosin, P. S.; Salzmann, R.; Togni, A. *J. Am. Chem. Soc.* **1994**, *116*, 4067−8. (c) Faller, J. W.; Mattina, M. J. *Inorg. Chem.* **1972**, *11*, 1296−307.
(18) Hayashi, T.; Yamamoto, A.; Iwata, T.; Ito, Y. *J. Chem. Soc., Chem. Commun.* **1987**, 398−9.
(19) (a) Braunschweig, H.; Dewhurst, R. D. *Dalton Trans.* **2011**, *40*, 549−58. (b) Amgoune, A.; Bourissou, D. *Chem. Commun.* **2011**, *47*, 859−71.
(20) Anderson, B. J.; Keith, J. A.; Sigman, M. S. *J. Am. Chem. Soc.* **2010**, *132*, 11872−4.
(21) Mesmer, R. E.; Rutenberg, A. C. *Inorg. Chem.* **1973**, *12*, 699−702.
(22) Ahijado Salomon, M.; Braun, T.; Penner, A. *Angew. Chem., Int. Ed.* **2008**, *47*, 8867−71.
(23) Wada, R.; Shibuguchi, T.; Makino, S.; Oisaki, K.; Kanai, M.; Shibasaki, M. *J. Am. Chem. Soc.* **2006**, *128*, 7687−91.
(24) (a) Kurosawa, H.; Ogoshi, S.; Kawasaki, Y.; Murai, S.; Miyoshi, M.; Ikeda, I. *J. Am. Chem. Soc.* **1990**, *112*, 2813−4. (b) Granberg, K. L.; Bäckvall, J. E. *J. Am. Chem. Soc.* **1992**, *114*, 6858−63.
(25) Emer, E.; Sinisi, R.; Capdevila, M. G.; Petruzziello, D.; De Vincentiis, F.; Cozzi, P. G. *Eur. J. Org. Chem.* **2011**, *2011*, 647−66.
(26) Strukul, G. *Top. Catal.* **2002**, *19*, 33−42.
(27) Lachance, H.; Hall, D. G. *Org. React. (Hoboken, NJ, U. S.)* **2008**, *73*, 1−573.